Angle-resolved photoemission study of a thin FeO(111) layer formed on Fe(110)

S. Masuda and Y. Harada
Department of Chemistry, College of Arts and Sciences, The University of Tokyo, Tokyo 153, Japan

H. Kato
Photon Factory, National Laboratory for High Energy Physics, Oho-machi, Ibaraki 305, Japan

K. Yagi
Institute of Physics, University of Tsukuba, Sakura-mura, Ibaraki 305, Japan

T. Komeda, T. Miyano,* M. Onchi, and Y. Sakisaka
Department of Chemistry, Faculty of Science, Kyoto University, Kyoto 606, Japan
(Received 28 August 1987)

The electronic properties of a thin FeO(111) layer epitaxially grown on Fe(110) have been studied by angle-resolved photoemission spectroscopy using polarized synchrotron radiation. The normal-emission spectra show five features: Fe $3d$-derived states at ~ 0.4 and 2.7 eV below the Fermi energy, O $2p$-derived states at ~ 4.1 and ~ 6.0 eV, and a multielectron satellite feature at 11.5 eV. The binding energies of these states were independent of $h\nu$ within ± 0.05 eV, in accord with the two-dimensionality of the layer. The band structure was mapped out in the two symmetry directions of the surface Brillouin zone: FeO[$1\bar{1}2$] ($\bar{\Gamma}\bar{M}$) and FeO[$1\bar{1}0$] ($\bar{\Gamma}\bar{K}$). The Fe $3d$-derived states show little dispersion ($\lesssim 0.2$ eV) with $\mathbf{k}_{\parallel}$, while the O $2p$-derived states exhibit considerable dispersion of ~ 2–3 eV in both directions. The dispersion of the O $2p$-derived bands can be understood in terms of a simple tight-binding model.

I. INTRODUCTION

The valence-electronic properties of transition-metal oxides with partially filled $3d$ states have been of great interest. The most essential question is why these materials are insulators (so-called Mott insulators) in contradiction to the naive band-theoretical point of view. So far, a large number of studies, both experimental[1–4] and theoretical,[5–10] have been performed.

In x-ray photoemission spectroscopy, the intensity of the O $2p$-derived features is weak, while the $3d$-derived features and multielectron satellite structure can be observed clearly. Hüfner and Wertheim[1] suggested that the $3d$-derived features can be identified as the ligand-field-split states of the $3d^{n-1}$ final configuration. The partial densities of states for the $2p$ and $3d$ bands in NiO, CoO, FeO, MnO, and Cr_2O_3 were determined by Eastman and Freeouf from photon-energy-dependent ($h\nu = 5$–90 eV) photoemission measurements.[2] They found that the $3d$ features are ~ 3 eV wide [full width at half maximum (FWHM)], located near the Fermi energy (E_F), and that the O $2p$ states are ~ 4 eV wide (FWHM), centered at ~ 3 eV below E_F, significantly overlapping with the $3d$ features in all cases. This overlap can lead to important physical consequences as it may imply a substantial contribution of a covalent nature to the crystal bonding. Furthermore, the recent resonant experiments on NiO (Refs. 3 and 4) showed the failure of the ligand-field theory to account for the satellite (owing to the effects of p-d mixing on a screening mechanism), and to explain the experiments a configuration-interaction (CI) model has been presented.[10] So far, the experimental studies have been focused mainly on the localized $3d$ states; the dispersive nature of the bandlike O $2p$ states still remains unclear, however. We note that for most transition-metal oxides an experimental electronic energy dispersion relation $E(\mathbf{k})$ is still missing, with the exception of a thin NiO(100) film formed on Ni(110).[11]

According to Ref. 12, well-ordered FeO is produced after oxygen exposure above 30 L (1 L $= 10^{-6}$ Torr sec) at 300 K, being oriented with FeO(111)||Fe(110), FeO[$1\bar{1}0$]||Fe[001], and FeO[$11\bar{2}$]||Fe[$1\bar{1}0$] (see Fig. 1). Figure 1 shows the two-dimensional atomic geometry (real space) and the Brillouin zone (BZ) (momentum space) for the FeO(111) layer formed on Fe(110). The lattice constant of the oxide layer has been evaluated to be 4.5 Å, which is $\sim 4\%$ larger than that of bulk FeO (4.31 Å).[12] FeO is an antiferromagnetic insulator with the NaCl structure ($T_N = 198$ K).

This paper is the second part of our photoemission work on the interaction of oxygen with a Fe(110) single-crystal surface. We performed angle-resolved photoemission measurements on a thin FeO(111) layer epitaxially formed on Fe($1\bar{1}0$) in order to clarify the dispersive nature of the valence states, especially the bandlike O $2p$ states. The results for clean Fe(110) (Ref. 13) and Fe(110)$c(2\times 2)$-O and Fe(110)$c(3\times 1)$-O chemisorption systems[14] have been reported.

II. EXPERIMENT

The Fe(110) crystal was cleaned by repeated Ar^+-ion sputtering and annealing cycles. The amounts of impuri-

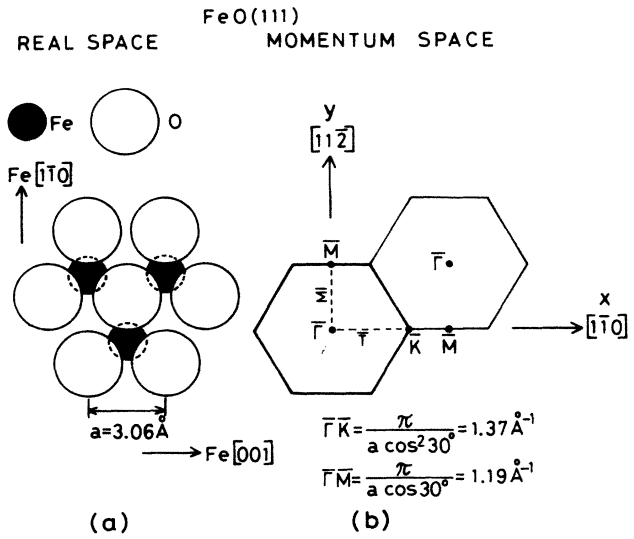

FIG. 1. (a) Real-space atomic geometry of the FeO(111) layer formed on Fe(110). (b) Surface Brillouin zone (SBZ) for the FeO(111) layer. The coordinate system is chosen such that the z axis is normal to the surface, and the x and y axes coincide with the crystallographic [1$\bar{1}$0] and [11$\bar{2}$] directions, respectively.

ties (S, Ar, C, N, and O) were reduced to less than the detection limit of Auger electron spectroscopy (AES) (i.e., $\lesssim 0.01$ monolayer). The clean Fe(110) surface showed a sharp $p(1\times1)$ low-energy electron-diffraction (LEED) pattern with a low background. The FeO(111) layer was prepared by exposing the clean surface to $\sim 5\times10^{-8}$ Torr oxygen at room temperature. The ordered structure of the oxide surface was verified by LEED. The photoemission experiments were performed at Photon Factory, National Laboratory for High Energy Physics, using a constant-deviation monochromator and a 150° spherical-sector-type analyzer with an acceptance angle of ±1°. The total experimental resolution was 0.3 eV. Charging problems did not occur for the samples of thin FeO films used. The base pressure in this system was 3×10^{-10} Torr. Details of the experimental setup and other related procedures were described elsewhere.[11,13,14]

III. RESULTS AND DISCUSSION

A. Coverage-dependent normal emission

Figure 2 shows the change in the normal-emission spectrum of a Fe(110) surface as a function of oxygen exposure up to 100 L at 300 K. All spectra were measured at a photon energy of $h\nu=40$ eV and at the angle of the light incidence of $\theta_i=25°$ (the surface component of the vector potential ($\mathbf{A}$) of the light was in the Fe[1$\bar{1}$0] azimuth, i.e., $\mathbf{A}_\parallel$ along Fe[1$\bar{1}$0]). Binding energy is referred to the Fermi energy (E_F) of the clean Fe(110) substrate. The clean-surface spectrum shows two structures at ~0.5 and 2.0 eV, which have been attributed to emissions from the 3d-like $\Sigma_1+\Sigma_4$ and Σ_4 bands, respectively.[15] As has been demonstrated in Ref. 13, contrary to

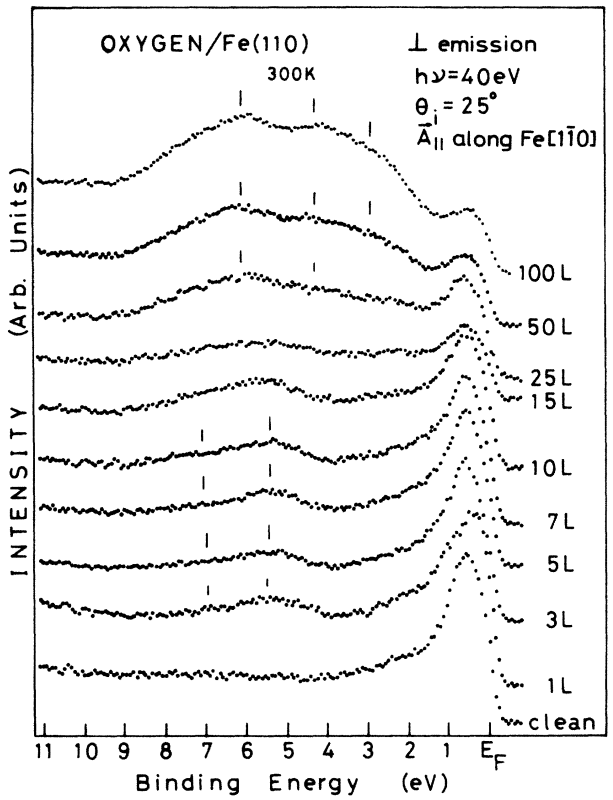

FIG. 2. Change in the normal-emission spectrum of the Fe(110) surface at $h\nu=40$ eV and 300 K as a function of oxygen exposure ($\theta_i=25°$, $\mathbf{A}_\parallel$ along [1$\bar{1}$0]).

the earlier observation of a satellite at ~5.5 eV,[16] no satellite feature is found for the "clean" surface.

For a small amount of oxygen exposure (around 1 L), two O 2p-derived peaks appeared at 5.5 and 7.0 eV below E_F. At ~2.5 and 6.5 L the $c(2\times2)$-O ($\frac{1}{4}$ monolayer) and $c(3\times1)$-O ($\frac{1}{3}$ monolayer) overlayers are formed, respectively,[12,14] and both peaks are scarcely shifted in energy ($\lesssim0.2$ eV) up to 10 L. These peaks are characteristic of dissociatively chemisorbed oxygen on Fe(110).[14] Between 10 and 15 L, the O 2p-derived peaks became broad and the Fe 3d emission just below E_F decreases in intensity rapidly. According to Ref. 17, these spectral changes are associated with the onset of oxygen incorporation into the selvage leading to the iron oxide formation (see also Ref. 12).

Beyond 30 L, the hexagonal LEED pattern was observed which ensures the epitaxial growth of FeO(111) on Fe(110).[12] The spectra of FeO(111) on Fe(110) exhibit new features at ~0.4, 2.7, ~4.1, and ~6.0 eV below E_F, and the lower-lying three peaks were developed with increasing exposure. The number and energies of peaks are in good agreement with the earlier results of the ultraviolet photoemission spectroscopy (UPS) studies on FeO.[2,17] The peaks at ~0.4 and 2.7 eV are ascribed to (or called) the Fe 3d emissions and the peaks at ~4.1 and ~6.0 eV to the O 2p emissions (these notations seem misleading if the 2p-3d hybridization is introduced). This assignment rests on the previous analysis of the photoemission spec-

trum of bulk FeO in terms of a ligand-field theory or very recent configuration-interaction theory (see Refs. 2 and 10). Previous AES and LEED study of the initial oxidation of Fe(110) has estimated the thickness of the oxide film, prepared by 100 L oxygen exposure at 300 K, to be 1.5–2 monolayers (4–5 Å) of FeO(111).[12] As the escape depth of photoelectrons with kinetic energy between ~40 and ~100 eV is established to be 4–5 Å in various materials, emissions from the underlying Fe substrate are expected to make an unimportant contribution to the spectrum of FeO(111) on Fe(110) (see also the results in Ref. 12).

Figure 3 shows the 3*p* core-level spectra for the clean Fe(110), oxygen-chemisorbed $c(3\times1)$ phase, and FeO(111) on Fe(110) measured at $h\nu=120$ eV. For Fe(110), the 3*p* emission lines are observed at ~53.6 ($3p_{1/2}$) and ~52.9 ($3p_{3/2}$) eV, whose averaged value is in good agreement with the x-ray photoemission spectroscopy (XPS) data (53±0.2 eV).[18] The binding energy is ~53.5 eV for the chemisorbed phase and is increased to ~56.0 ($3p_{1/2}$) and ~54.5 ($3p_{3/2}$) eV for the oxide. These data show the potential of the 3*p* core level for surface-compound identification in a fingerprinting way [electron spectroscopy for chemical analysis (ESCA)]. The difference in these chemical shifts can be attributed primarily to that in the Fe valences (3*d*-electron occupation numbers). The 3*p* levels for Fe metal ($3d^74s$ configuration) can be expected to have lower binding energy than those for the Fe^{2+} ion ($3d^6$ configuration) in FeO because of the screening by the extra 3*d* electron. Thus the Fe 3*p* binding energy increases in the order $Fe^0 < Fe^{2+}$ simply because of the final-state relaxation and the increasingly attractive core potential, though it is not trivial since the Madelung potential effects should also be considered. It is also interesting that the apparent spin-orbit splitting between the $3p_{1/2}$ and $3p_{3/2}$ peaks varies for different Fe valences. It is estimated to be ~0.7 eV for the metal and is increased to ~1.5 eV for the oxide. Similar phenomena have been observed for the 2*p* core levels of 3*d* transition-metal compounds,[19,20] where the spin-orbit splitting between the $2p_{1/2}$ and $2p_{3/2}$ peaks is found to be larger than that of metal by 1 to 2 eV for compounds with larger uncompensated spins. This increase in splitting was attributed to the exchange interaction between the spins of 2*p* hole and 3*d* electrons and/or to the reduced screening of the nuclear Coulomb potential by 3*d* electrons.

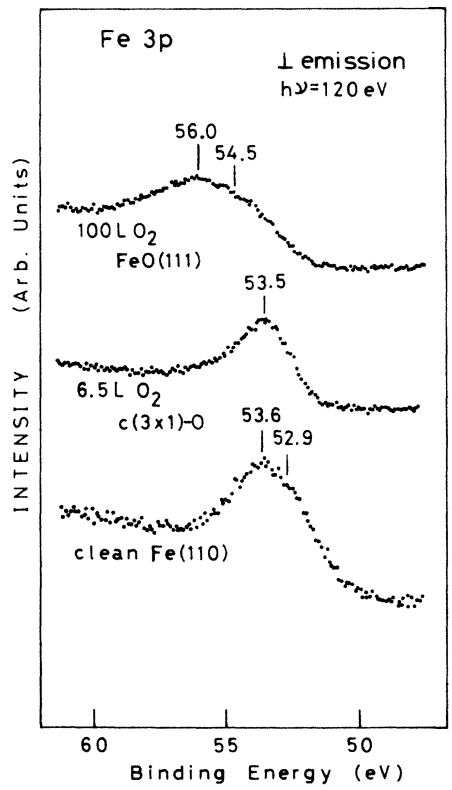

FIG. 3. Fe 3*p* spectra for the clean Fe(110), oxygen-chemisorbed $c(3\times1)$ phase, and FeO(111) on Fe(110).

B. Photon-energy dependence

Figure 4 shows the $h\nu$ dependence of the normal-emission spectrum of FeO(111) on Fe(110) prepared by 100 L oxygen exposure at 300 K. The oxygen-derived

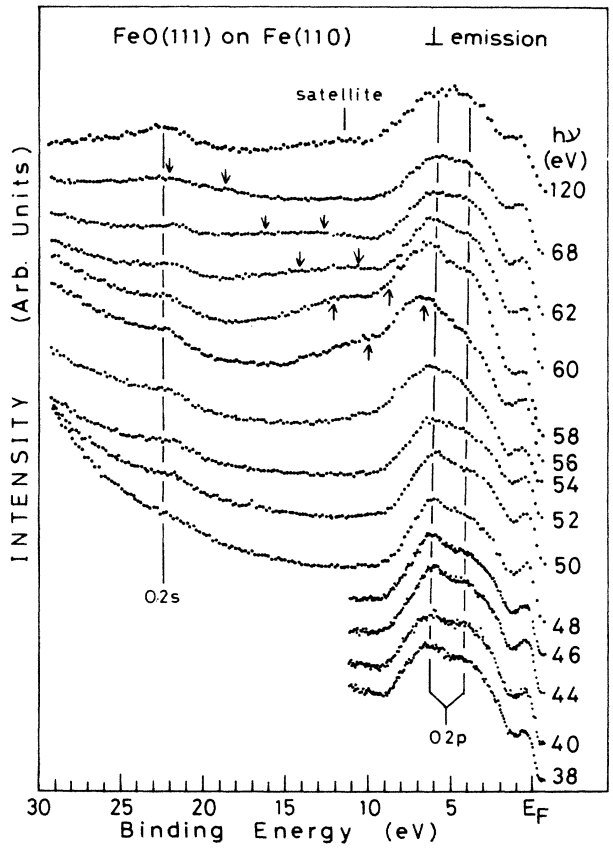

FIG. 4. $h\nu$ dependence of normal-emission spectra for the FeO(111) on Fe(110) prepared by 100 L oxygen exposure at 300 K. The O 2*s*– and 2*p*–derived states are indicated by vertical lines. The expected positions of the $M_{2,3}VV$ SCK lines are indicated by arrows.

states are indicated by vertical lines. The arrows indicate the expected peak positions of the ordinary $M_{2,3}VV$ super-Coster-Kronig (SCK) emissions which have constant kinetic energies of 47 and 50 eV (referred to E_F).[21] As expected from the fact that the FeO(111) layer is thin [1.5–2 FeO(111) planes], i.e., there is no periodicity along the in-depth direction, the O $2p$–derived states stay at fixed binding energies within ± 0.05 eV when the photon energy is changed. Therefore these states can be ascribed to the two-dimensional ones. The weak valence-band satellite at 11.5 eV below E_F is seen for $h\nu \gtrsim 68$ eV but not for the excitation energy below the $3p$ threshold (between $h\nu = 62$ and 56 eV, whether the satellite exists is not clear because of the overlap of the SCK emissions). This result exhibits a striking contrast to those of bulk NiO (Refs. 3 and 4) and NiO formed on Ni(110),[11] in which the satellite is clearly observed even for the low-energy excitation and shows a strong resonant behavior at the $3p$ threshold.

C. Incidence angle dependence

Figure 5 shows normal-emission spectra of FeO(111) formed on Fe(110), which was prepared by 100 L oxygen exposure at 300 K, measured at two angles of the light incidence of $\theta_i = 50°$ [with both $\mathbf{A}_\parallel$ (parallel to the surface) and $\mathbf{A}_\perp$ (perpendicular to the surface) components of $\mathbf{A}$] and 25° (with predominant $\mathbf{A}_\parallel$ and small $\mathbf{A}_\perp$ components). The component $\mathbf{A}_\parallel$ is oriented parallel to the FeO[$1\bar{1}0$] direction and the photon energy is $h\nu = 40$ eV.

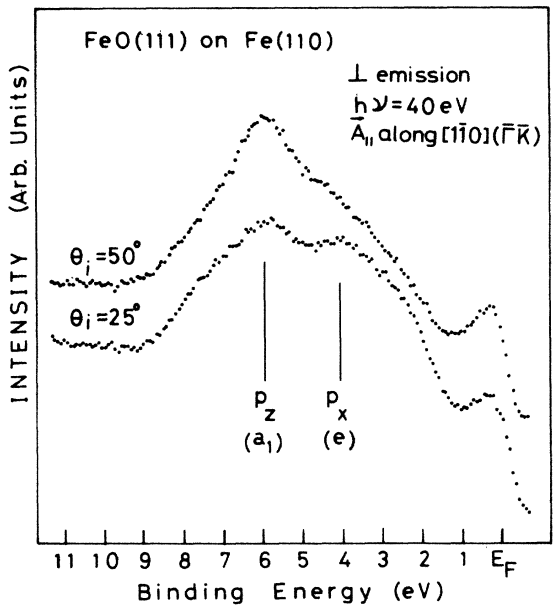

FIG. 5. Normal-emission spectra for FeO(111) formed on Fe(110) (prepared by 100 L oxygen exposure at 300 K) at two angles of the light incidence of $\theta_i = 25°$ and 50°. The photon energy is 40 eV and the component of the polarization vector $\mathbf{A}$ parallel to the surface is along the [$1\bar{1}0$] direction. The O $2p$–derived emission features are indicated by vertical bars.

Figure 6 also shows normal emission except that the sample has been rotated 90° until the parallel component $\mathbf{A}_\parallel$ is along the FeO[$11\bar{2}$] direction. Two oxygen-derived peaks indicated by vertical bars are seen in each figure. Both peaks are observed for $\theta_i = 50°$, while the higher-binding-energy peak at ~ 6.0 eV is reduced in intensity as compared with the ~ 4.1-eV peak for $\theta_i = 25°$.

The symmetry of the O $2p$–derived states can be identified in normal-emission collection ($\mathbf{k}_\parallel = 0$ or $\bar{\Gamma}$). Since the states at the $\bar{\Gamma}$ point have C_{3v} symmetry, the O $2p$ orbitals will form two types of molecular orbitals with Fe orbitals if the electronic states of FeO are discussed in terms of a tight-binding scheme: The orbital with an a_1 symmetry is constructed from the O $2p_z$ (z: normal to the surface) orbitals, whereas the degenerated e orbitals are constructed from the O $2p_x$ and O $2p_y$ orbitals (see the coordinate system of Fig. 1). The final state, which is an outgoing wave to the detector, has a_1 symmetry. The polarization vector perpendicular (parallel) to the surface, $\mathbf{A}_\perp$ ($\mathbf{A}_\parallel$), can excite only an a_1- (e-) symmetry initial state in the normal-emission collection. If $\mathbf{A}$ is perfectly parallel to the surface and also to the x or y axis (i.e., the collection mirror plane) only the even e state (O p_x or O p_y) can be observed. Therefore the FeO(111) spectra in Figs. 5 and 6 indicate that the O $2p_z$ (a_1) level is at ~ 6.0 eV below E_F and the O $2p_x p_y$ (e) level is at ~ 4.1 eV.

D. Off-normal emission and the band structure

Detailed information on the electronic properties of FeO(111) can be obtained by evaluating the energy-band dispersion. Figures 7 and 8 show examples of angle-resolved photoemission spectra taken at different emis-

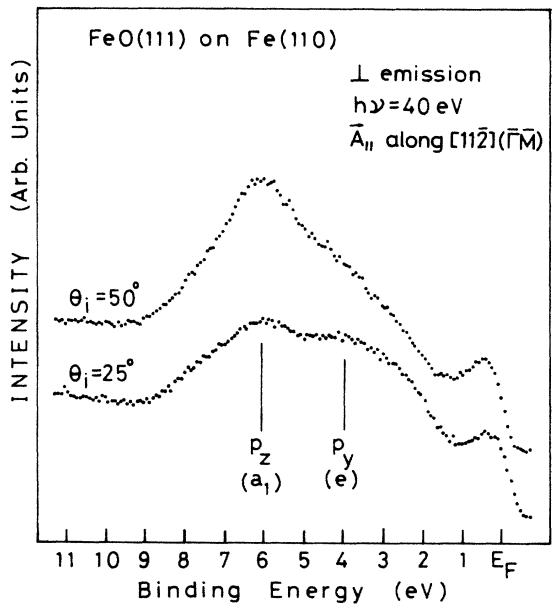

FIG. 6. Normal-emission spectra for FeO(111) on Fe(110). The details are the same as in Fig. 5 except that $\mathbf{A}_\parallel$ is now in the [$11\bar{2}$] direction.

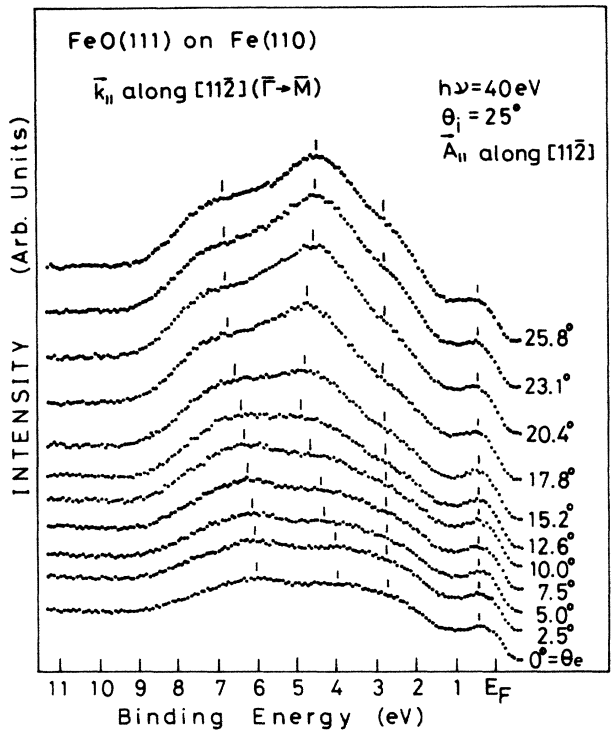

FIG. 7. Angle-resolved photoemission spectra for FeO(111) on Fe(110) measured at $h\nu=40$ eV and $\theta_i=25°$ in the [11$\bar{2}$] ($\bar{\Gamma}\,\bar{M}$) direction ($\mathbf{A}_{\parallel}$ along [11$\bar{2}$]). The emission angle θ_e is indicated on the right-hand side of each spectrum. The positions of the spectral structures are indicated by vertical bars.

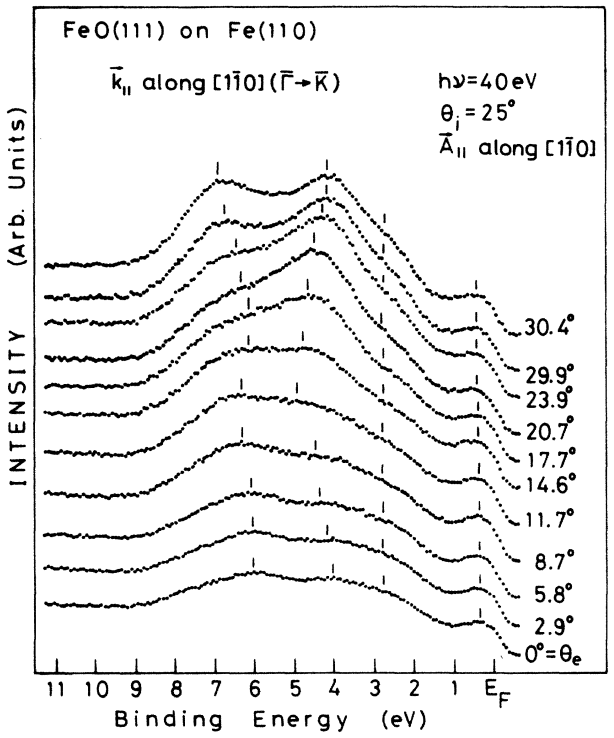

FIG. 8. Angle-resolved photoemission spectra for FeO(111) on Fe(110) measured at $h\nu=40$ eV and $\theta_i=25°$ in the [1$\bar{1}$0] ($\bar{\Gamma}\,\bar{K}$) direction ($\mathbf{A}_{\parallel}$ along [1$\bar{1}$0]). The emission angle θ_e is indicated on the right-hand side of each spectrum. The positions of the spectral structures are indicated by vertical bars.

sion angles (θ_e) in the two symmetry directions of the FeO(111) surface Brillouin zone (SBZ). All spectra were taken at $h\nu=40$ eV and at $\theta_i=25°$ with the polarization vector in each collection plane. The emission angle θ_e is indicated on the right-hand side of each spectrum. The positions of the structures in the FeO(111) spectra were determined by comparing the $\theta_i=25°$ and $\theta_i=60°$ spectra (e.g., see Figs. 5 and 6) and referring to other sets of the $\theta_i=25°$ spectra (not shown). The resulting positions are indicated by vertical bars.

The band structure $E(\mathbf{k}_{\parallel})$ can be directly mapped out using the relation between the parallel component of the detected wave vector ($\mathbf{k}_{\parallel}$) and the measured kinetic energy ($E_{\rm kin}$), i.e.,

$$\mathbf{k}_{\parallel}=[(2m/\hbar^2)E_{\rm kin}]^{1/2}\sin\theta_e \ .$$

The work function of the FeO(111) film used has been evaluated to be $\sim$4.5 eV.[12] The results are summarized in Fig. 9 for the two symmetry directions $\bar{\Gamma}\,\bar{K}$ and $\bar{\Gamma}\,\bar{M}$ of the FeO(111) SBZ. In the figure the experimental points are represented by dots. It can be easily seen that the higher-lying Fe 3*d* states show little dispersion ($\lesssim$0.2 eV), while the lower-lying O 2*p* states exhibit a considerable dispersion ($\sim$2–3 eV) in both directions. This behavior is consistent with the hybrid model proposed by Adler and Feinleib for the electronic structures of transition-metal oxides.[5]

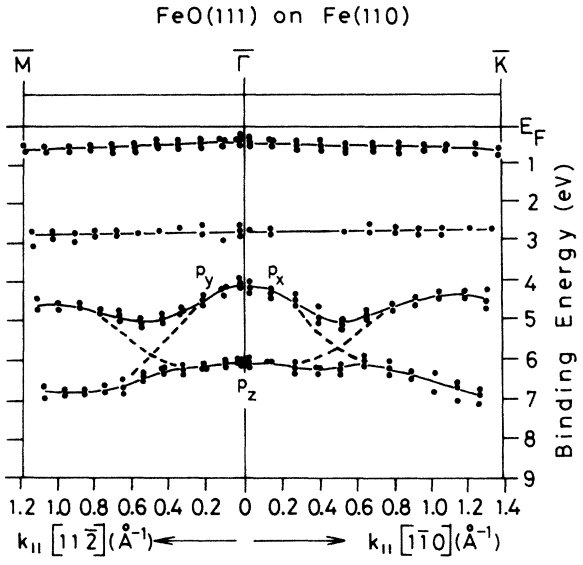

FIG. 9. Measured dispersion $E(\mathbf{k}_{\parallel})$ of the valence states for FeO(111) on Fe(110) in the symmetry directions $\bar{\Gamma}\,\bar{M}$ and $\bar{\Gamma}\,\bar{K}$ of the SBZ. The experimental points are indicated by dots. The dashed lines represent the O 2*p*–derived band without hybridization (see text).

As indicated in Fig. 1, the FeO(111) layer has an only mirror plane in the $[11\bar{2}]$ direction [$(1\bar{1}0)$ mirror plane]. Since the present measurements were performed with the light polarization in the collection plane, only even states could be observed owing to the symmetry selection rules. In the $(1\bar{1}0)$ mirror plane (along $[11\bar{2}]$), the $p_x p_y$ states split into two bands, one an even- and the other an odd-state band with respect to the reflection on the mirror plane. The p_z band has an even symmetry. Accordingly, the two even bands always could be observed in the even collection geometry. On the other hand, the situation is different in the case of the $(11\bar{2})$ plane (along $[1\bar{1}0]$), because the $(11\bar{2})$ plane is not a mirror plane. Therefore, in principle all three bands should be observed (as a matter of fact, as discussed below, only the two O $2p$ peaks were observed).

In the $[11\bar{2}]$ direction, two O $2p$-derived states were observed: the lower O $2p$-derived band (6.0 eV at $\bar{\Gamma}$) disperses to higher binding energy (downward) by ~ 0.7 eV with increasing $\mathbf{k}_\parallel$ up to 1.19 Å^{-1} (i.e., $\bar{M}$), while the upper O $2p$-derived band (4.1 eV at $\bar{\Gamma}$) shifts from 4.1 to 5.0 eV with increasing $\mathbf{k}_\parallel$ up to ~ 0.5 Å^{-1} and then toward lower binding energy in the region $\mathbf{k}_\parallel \geq 0.5$ Å^{-1} [4.6 eV at $\mathbf{k}_\parallel = 1.19$ Å^{-1} ($\bar{M}$)]. On the other hand, in the $[1\bar{1}0]$ ($\bar{\Gamma}\bar{K}$) direction we observed only two O $2p$-derived states (see Fig. 9): The lower band disperses downward by ~ 0.8 eV with increasing $\mathbf{k}_\parallel$ up to 1.37 Å^{-1} (i.e., $\bar{\Gamma}\bar{K}$), whereas the upper band shifts from 4.1 to 5.0 eV up to $\mathbf{k}_\parallel = 0.5$ Å^{-1} and then toward lower binding energy in the region $\mathbf{k}_\parallel \geq 0.5$ Å^{-1} [4.3 eV at $\mathbf{k}_\parallel = 1.37$ Å^{-1} ($\bar{K}$)]. These findings suggest that angle-resolved photoemission spectroscopy is rather insensitive to multiple scattering in the final state between adsorbate [in this case, O ions in FeO(111)] and substrate [the underlying Fe ions in FeO(111)] and therefore is dominated by the symmetry of the O-ion layer. If multiple scattering were relevant, the selection rules for emission should be led from the symmetry of the whole system [O-ion layer, Fe-ion layer, and Fe(110)]. We found that this is not the case.

In order to understand the dispersive behavior of the O $2p$-derived states, we tried to predict a qualitative band structure for an unsupported two-dimensional hexagonal oxygen-ion layer (D_{6h} symmetry) on the basis of a simple tight-binding concept. A similar argument has been made for hexagonal chalcogen overlayers on Al(111) (Ref. 22) and oxygen overlayers on Fe(110).[14] Figure 10 shows the real parts of the p_x, p_y, and p_z wave functions in the real-space representation for the isolated hexagonal oxygen-ion layer at three different wave vectors in the $\bar{\Gamma}\bar{M}$ and $\bar{\Gamma}\bar{K}$ directions. Because both directions involve the mirror planes of the oxygen-ion layer, all wave functions are even or odd.

At $\bar{\Gamma}$ ($\mathbf{k}_\parallel = 0$), all the wave functions at the neighboring lattice sites are in phase. Therefore, the p_z state has a complete bonding character while the degenerate p_x and p_y states have antibonding nature. At $\bar{M}$, all rows of ions perpendicular to $\mathbf{k}_\parallel$ have the same phase but each row has a phase change of π. Figure 10 shows that at $\bar{M}$ the even p_z state is antibonding because each ion is surrounded by four ions of opposite phase and two ions being in phase. On the other hand, the odd p_x and even p_y states become more bonding in character. Therefore, the even p_z state should disperse upward from $\bar{\Gamma}$ to $\bar{M}$, and the odd p_x and even p_y states downward from $\bar{\Gamma}$ to $\bar{M}$. The behavior in the $[1\bar{1}0]$ direction is quite different. At $\bar{K}$ ($\mathbf{k}_\parallel = 4\pi/3a$), $\mathbf{k}(\bar{K})/\pi$ is not an integral multiple of the inverse of the row spacing in this direction ($a/2$). Therefore we consider the phase of the wave functions at $\mathbf{k}_\parallel = 0.75\mathbf{k}(\bar{K}) = \pi/a$, where each row of lattice sites perpendicular to $\mathbf{k}_\parallel$ is out of phase with the adjacent row by $\pi/2$ so that the amplitude of the phase is $+1$, 0, -1, 0, $+1$, etc. The sites with zero phase are represented by small dots in Fig. 10. At $\mathbf{k}_\parallel = 0.75\mathbf{k}(\bar{K})$, the even p_z state is strongly antibonding, while the even p_x and odd p_y states become bonding. The wave functions at $\mathbf{k}_\parallel = 1.5\mathbf{k}(\bar{K})$ are the same as those at $\bar{M}$ in the second zone. The predicted dispersion thus obtained is shown schematically at the bottom of Fig. 10. The even bands are represented by solid lines and the odd bands by dashed lines. Similar dispersion was obtained by the cal-

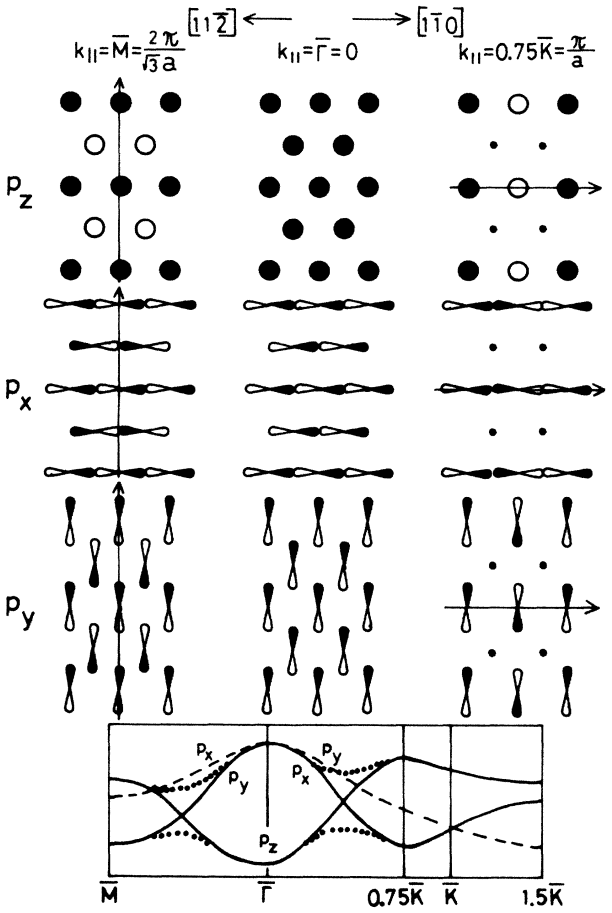

FIG. 10. Schematic representation of the p_x, p_y, and p_z wave functions for an isolated oxygen-ion layer at three different values of $\mathbf{k}_\parallel$ in the $\bar{\Gamma}\bar{M}$ and $\bar{\Gamma}\bar{K}$ directions in the SBZ. The arrows indicate the direction of $\mathbf{k}_\parallel$. The bottom figure shows the dispersion expected by a tight-binding approximation.

culation for the same isolated system using an LCAO-$X\alpha$-SCF method.[23]

When this hexagonal (1×1) oxygen-ion layer is placed in contact with the "unstructured" Fe-ion layer, the symmetry of the layer is reduced from D_{6h} to C_{6v} (due to the break in the reflection symmetry about the central plane of the two-dimensional oxygen-ion layer). Therefore the two even states (with respect to the mirror plane symmetry) will hybridize with each other at the crossing points, forming a gap. This is illustrated schematically by the dotted lines in Fig. 10 (bottom).

From the comparison between Figs. 9 and 10, the overall trend and the qualitative features of the experimental results are found to be well reproduced by the energy dispersion based on the concept of a simple tight-binding approach. In particular, it is clearly seen that hybridization occurs both in the $\bar{\Gamma}\bar{M}$ and $\bar{\Gamma}\bar{K}$ directions because of the crossing of the even bands. The dashed lines in Fig. 9 show what the bands could have looked like before hybridization. The analysis of the data indicates that the p_z band disperses by ~1.5 eV and the p_x and p_y band by ~2.7 eV before hybridization. Since the distance between oxygen ions for the FeO(111) layer, 3.06 Å, is close to the O^{2-} ion diameter (2.80 Å), a large dispersion of the O $2p$-derived states can be expected by the direct overlap between the wave functions of the nearest-neighbor oxygen ions.

In the thin layer the number of neighbors is reduced as compared to the bulk, and since the bandwidth is proportional to the number of neighbors in a nearest-neighbor approximation for a single band, a narrowing of the band should be expected. As seen in Fig. 9, the observed O p_z and O p_xp_y are separated at $\bar{\Gamma}$. Therefore, even if we take the above narrowing effect into account, the measured dispersion for FeO(111) on Fe(110) cannot be compared directly with the band structure of bulk FeO. However, we find our results consistent with the hybrid model of Adler and Feinleib[5] where the $2p$ orbitals form a wide band and the $3d$ levels form localized states. This model was not rigorously related to a quantum-mechanical Hamiltonian and its parameterization is fully empirical. So far, the band-structure calculations for bulk FeO have been performed by Mattheiss[6] and Kunz and Surratt.[7] The calculations of Mattheiss employ the Slater exchange (local density) approximation and are non-self-consistent. On the other hand, Kunz and Surratt included correlation effects in a self-consistent restricted Hartree-Fock energy calculation and in this case the inclusion of correlation corrections was found to substantially modify the energy-band structure. They reported the energy bands of FeO along the ΓX direction in the bulk BZ. We note that the bands of Kunz and Surratt are consistent with the model of Adler and Feinleib[5] concerning the localized $3d$ levels as well as the broad $2p$ bands (also see Fig. 9). However, this does not mean the success of the band theory for FeO, since, e.g., the band theory in which exchange and correlation effects are replaced by effective one-particle potentials never explains the insulating nature of FeO [the observed band gap of 2.8 eV (Ref. 24)]. Some authors[9] concluded that the failure of the conventional band theory is ascribed to the local-density approximation for exchange and correlation.

IV. SUMMARY

Angle-resolved photoemission measurements have been performed on a thin FeO(111) layer formed on Fe(110) and the two-dimensional band dispersion was mapped out in the two symmetry directions of the surface BZ (i.e., FeO[11$\bar{2}$] ($\bar{\Gamma}\bar{M}$) and FeO[1$\bar{1}$0] ($\bar{\Gamma}\bar{K}$)). The Fe $3d$-derived states show little dispersion ($\lesssim0.2$ eV), whereas the O $2p$-derived states exhibit considerable dispersion of $\sim2-3$ eV in both directions. The dispersive features of the O $2p$-derived states are qualitatively reproduced by the band structure predicted for a two-dimensional isolated oxygen monolayer in a simple tight-binding model. In order to yield a quantitative description including the estimates of the band position and width, etc., the model should be improved by considering the change in the oxygen-ion wave functions due to the mixing of Fe $3d$ electrons. Our experimental results including Fe $3d$ states will provide useful information on band calculations for transition-metal oxides.

ACKNOWLEDGMENTS

We are pleased to thank the staff of Photon Factory, National Laboratory for High Energy Physics, particularly Dr. T. Miyahara, for their excellent support. One of us (S.M.) thanks Dr. M. Tsukada and Dr. N. Shima for helpful discussion. This work has been performed under the approval of the Photon Factory Program Advisory Committee (Proposal No. 84-080).

*Present address: Opto-electronics R & D Laboratories, Sumitomo Electric Industries Ltd., Yokohama 244, Japan.

[1]S. Hüfner and G. K. Wertheim, Phys. Rev. B **8**, 4857 (1973).
[2]D. E. Eastman and J. L. Freeouf, Phys. Rev. Lett. **34**, 395 (1975).
[3]S. J. Oh, J. W. Allen, I. Lindau, and J. C. Mikkelsen, Jr., Phys. Rev. B **26**, 4845 (1982).
[4]M. R. Thuler, R. L. Benbow, and Z. Hurych, Phys. Rev. B **27**, 2082 (1983).
[5]D. Adler and J. Feinleib, Phys. Rev. B **2**, 3112 (1970).
[6]L. F. Mattheiss, Phys. Rev. B **5**, 290 (1972).
[7]A. B. Kunz and G. T. Surratt, Solid State Commun. **25**, 9 (1978); A. B. Kunz, J. Phys. C **14**, L455 (1981).
[8]K. H. Johnson, R. P. Messmer, and J. W. D. Connolly, Solid State Commun. **12**, 313 (1973).
[9]K. Terakura, T. Oguchi, A. R. Williams, and J. Kübler, Phys. Rev. B **30**, 4734 (1984).
[10]A. Fujimori, F. Minami, and S. Sugano, Phys. Rev. B **29**, 5225 (1984).
[11]T. Komeda, Y. Sakisaka, M. Onchi, H. Kato, S. Masuda, and K. Yagi, Surf. Sci. (to be published).
[12]C. Leygraf and S. Ekelund, Surf. Sci. **40**, 609 (1973); T. Mi-

yano, Y. Sakisaka, T. Komeda, and M. Onchi, *ibid.* **169**, 197 (1986).

[13]H. Kato, T. Ishii, S. Masuda, Y. Harada, T. Miyano, T. Komeda, M. Onchi, and Y. Sakisaka, Phys. Rev. B **32**, 1992 (1985); **34**, 8973 (1986).

[14]Y. Sakisaka, T. Komeda, T. Miyano, M. Onchi, S. Masuda, Y. Harada, K. Yagi, and H. Kato, Surf. Sci. **164**, 220 (1985).

[15]Y. Sakisaka, T. Rhodin, and D. Mueller, Solid State Commun. **53**, 793 (1985).

[16]D. Chandesris, J. Lecante, and Y. Petroff, Phys. Rev. B **27**, 2630 (1983); **34**, 8971 (1986).

[17]G. Pirug, G. Brodén, and H. P. Bonzel, Surf. Sci. **94**, 323 (1980).

[18]See, e.g., the table of core-level binding energies in *Photoemission in Solids II*, Vol. 2 of *Topics in Applied Physics*, edited by L. Ley and M. Cardona (Springer, Berlin, 1979).

[19]D. C. Frost, C. A. McDowell, and I. S. Woolsey, Chem. Phys. Lett. **17**, 320 (1972).

[20]S. P. Kowalczyk, L. Ley, F. R. McFeely, and D. A. Shirley, Phys. Rev. B **11**, 1721 (1975).

[21]Y. Sakisaka, T. Miyano, and M. Onchi, Phys. Rev. Lett. **54**, 714 (1985).

[22]P. Hofmann, C. v. Muschwitz, K. Horn, K. Jacobi, A. M. Bradshaw, and K. Kambe, Surf. Sci. **89**, 327 (1979); K. Jacobi, C. v. Muschwitz, and K. Kambe, *ibid.* **93**, 310 (1980).

[23]M. Tsukada and N. Shima (private communication).

[24]H. K. Bowen, D. Adler, and B. H. Auker, J. Solid State Chem. **12**, 355 (1975).